Construction and Building Materials 499 (2025) 144111

Contents lists available at ScienceDirect

Construction and Building Materials

journal homepage: www.elsevier.com/locate/conbuildmat

Effect of content, gradation, and saturation of expanded waste glass aggregates on physical and mechanical properties of a fly-ash geopolymeric mortar

Emilia Vasanelli [a,*], Silvia Calò [b], Marianovella Leone [b], Maria Antonietta Aiello [b]

[a] National Research Council (CNR) - Institute of Heritage Science (ISPC), Prov. le Lecce-Monteroni, Lecce 73100, Italy
[b] Department of Innovation Engineering, University of Salento, University Campus, Prov. le Lecce-Monteroni, Lecce 73100, Italy

ARTICLE INFO

Keywords:
Waste glass expanded aggregates
Fly ash geopolymer
Lightweight aggregates
Sustainable mortars
Lightweight aggregates prewetting

ABSTRACT

With low density, high mechanical strength, and high frost resistance, expanded waste glass aggregates (EWGA) can be a promising ecological solution as lightweight aggregates in concrete and mortars. Using a geopolimeric matrix, instead of OPC, could enhance material durability and environmental sustainability by employing waste materials in both the aggregates and the matrix. In the present paper, EWGAs were added to fly ash geopolymeric mortars. The effects of aggregate parameters, namely saturation degree, amount, and gradation, were analyzed. All these factors resulted in varying fluid absorption by aggregates during mortar mixing, leading to different final properties of the materials. The impact of liquid absorption by LWA has been extensively studied in OPC concrete and mortars, but limited research exists regarding geopolymers. This work aims to expand the knowledge of EWGA behavior in geopolymers, proposing strategies for mix design optimization with the ultimate scope of promoting the employment of waste materials in building technology. UPV, weight monitoring, and morphological analysis by SEM were performed to investigate the effects of EWGA parameters on the progress of geopolymerization reactions. Key physical and mechanical properties—including bulk density, total porosity, UPV, compressive/flexural strengths, and thermal conductivity—were evaluated to establish the relationship between EWGA characteristics and the overall performance of the geopolymeric composites. Experimental results highlighted that prewetting aggregates allowed for reducing the alkaline solution (AAS) content in the mortars and, at the same time, for obtaining the same mechanical performances as dry aggregate mortars, reducing density (13 %), thermal conductivity (20 %), and polymerization time. Reducing the content of the alkaline solution in the mix is noteworthy, as it is costly and environmentally impactful. The experimental results also evidenced the critical role of the fine fraction of EWGA in both the geopolymerization process and final mortar properties (lowering of flexural and compressive strength of 40 % and 10 %, respectively, in absence of fines), and the positive effects of increasing the content of EWGA on the mechanical properties (strength increase of 25 % in bending and 10 % in compression) and thermal conductivity (6 % reduction).

1. Introduction

Lightweight aggregates (LWA) are commonly utilized to reduce the apparent density of concrete and mortars and consequently the dead loads of structures, ensuring at the same time higher thermal and acoustic insulation, and higher fire resistance [1]. Lightweight aggregate concrete traces back to 3000 years ago when volcanic materials were used as lightweight aggregates [2]. LWA can be classified into two categories, namely natural (found in the environment with little to no change needed) and artificial (a by-product of heat treatment of expansive materials or a manufactured product entirely) [3]. Artificial lightweight aggregates produced from waste materials are an environmentally friendly and economical solution. In the last years, extensive research has been devoted to the use of lightweight and normal waste aggregates in the substitution of natural ones, aiming at lowering the continuous depletion of natural resources by concrete and mortar production [4]. Plastic [5], construction and demolition [6], rock dust [7] waste as normal aggregate, and palm oil, expanded clay, and lava [8] as

* Corresponding author.
E-mail addresses: emilia.vasanelli@cnr.it (E. Vasanelli), silvia.calo@unisalento.it (S. Calò), marianovella.leone@unisalento.it (M. Leone), antonietta.aiello@unisalento.it (M.A. Aiello).

https://doi.org/10.1016/j.conbuildmat.2025.144111
Received 24 June 2025; Received in revised form 22 September 2025; Accepted 17 October 2025
Available online 23 October 2025

LWA are only examples of waste aggregate materials.

With low density, high mechanical strength, and high frost resistance, expanded waste glass aggregates (EWGA) can be a promising ecological solution as LWA in concrete [9]. EWGA employment in concrete can further push recycling waste glass, obtaining several well-known environmental benefits [10]. Indeed, globally, around 130 million tons of glass are produced annually, among which approximately 100 million tons are discarded as waste [11]. It is estimated that recycling glass allowed: 1) savings in raw materials: over a ton of natural resources are conserved for every ton of glass recycled; 2) a decrease in energy use: 2–3 % drop in cost for every 10 % cullet used in the manufacturing process; 3) greenhouse gas reduction: a ton of carbon dioxide is reduced for every 6 tons of recycled container glass; 4) no processing by-products: glass recycling is a closed-loop system, creating no additional waste or by-products [12]. EWGAs are obtained by mixing finely ground recycled waste glass with appropriate expansive agents (such as $MgCO_3$, $CaCO_3$, SiC, black carbon, poly methyl methacrylate) and firing it at high temperatures up to the softening point of glass (typically 900–1300 °C) [9,13,14]. Water absorption, density, and strength are the most prominent properties of EWGA [4]. The characteristics and performance of expanded glass aggregates are highly dependent on their cell size, which in turn depends on the foaming agent particle size, quantity, time, and heating temperature. The greater the size of EWGA cells, the lower their density, thermal conductivity, and mechanical performance. On the contrary, EWGA particles of smaller size have high-strength properties with increased density and thermal conductivity [14]. Literature studies show that the water absorption of expanded glass aggregates varies with their particle size. It can vary up to 25 % [9]. This aspect strongly influences the concrete mix design and the material performances in fresh and hardened states.

The main concern in using EWGA in concrete is the possibility of the alkali-silica reaction (ASR). The amorphous silica in the aggregates can react with the alkaline environment of concrete, leading to the formation of expansive products that can damage the material [15]. Most literature studies regarding using EWGA in concrete focus on this issue [16]. Research findings are contradictory [9,17], stating that the ASR does not appear [18], appears without causing any damage as the ASR products are formed in the pores [13,19], or appears and causes structural damage [20]. ASR can be overcome if a geopolymeric matrix is used to substitute cement (OPC), as demonstrated by several studies in the literature [21–23]. A geopolymer is obtained through a polymerization process, starting from natural or waste materials with a high content of aluminum or silicon (precursors) [24,25]. The reaction between the precursor powder and an alkaline activating solution (AAS) produces a strong inorganic polymer, which is used as the binder in concrete and mortars. The impact of the alkali-silica reaction is minimal in geopolymers due to their lower calcium content, compared to the OPC matrix (especially when fly ash geopolymers are used), and because most of the alkalis were consumed during the geopolymerization reactions [22,23]. Additionally, geopolymers have been proposed as a green and sustainable alternative to ordinary Portland cement, thereby significantly reducing their environmental footprint. They represent an innovative challenge for producing new building materials, lowering consumption during production, minimizing greenhouse gas emissions, and lessening environmental impact [26–29]. Therefore, using EWGA as aggregates in concrete/mortars, coupled with a geopolymer matrix instead of the conventional cement matrix, could address durability concerns related to the alkali-silica reaction while also enhancing environmental sustainability.

In the present paper, waste glass expanded aggregates were added to fly ash geopolymeric mortars. The paper aimed to evaluate the influence of different EWGA parameters on the geopolymers' final physical/mechanical properties. The scope was to contribute to deepening the knowledge about EWGA employment within geopolymers, aiming to spread the use of these waste materials in building technology. The saturation degree of aggregates, their amount, and grading were the analyzed parameters. All these factors caused different liquid absorption by aggregates during mortar mixing and, thus, different final properties of the materials. The effect of fluid absorption by LWA on mixing and final concrete/mortar properties has been widely studied in OPC concrete/mortars, and several mix design strategies have been proposed in the literature [30–32]. On the contrary, LWA liquid absorption has been poorly studied when the binder is a geopolymer [3]. Indeed, the aggregate absorption behavior and its effect should be different from that of OPC concrete because the activator is different. It is water in the case of OPC, while it is the alkaline solution in geopolymers, which is indispensable to start geopolymerization reactions. When EWGAs are added to the mix at ambient conditions, part of the AAS is absorbed by aggregates [33–35]. Thus, it can be assumed that only part of the solution effectively causes the geopolymerization reactions, as the remaining part wets the aggregates and ensures the necessary workability of the mix [35]. This circumstance is anti-economic if it is considered that the alkaline solution is expensive and has a high impact on the total cost of the material. Thus, reducing its use in geopolymers is a challenge.

To comprehensively assess the influence of expanded waste glass aggregate (EWGA) characteristics on the performance of geopolymeric mortars, seven mixes were developed to investigate the contribution of EWGA amount, grading, and degree of saturation to AAS absorption and mortar final properties. The progress of geopolymerization in the mortars was monitored through ultrasonic pulse velocity (UPV) measurements and mass variation over time. Additionally, scanning electron microscopy (SEM) was employed to examine the microstructural morphology of the hardened mortars. Key physical and mechanical properties—including bulk density, total porosity, UPV, compressive/flexural strengths, and thermal conductivity—were evaluated to establish the relationship between EWGA characteristics and the overall performance of the geopolymeric composites. This study contributes to the optimization of mix design strategies for sustainable geopolymer-based materials incorporating expanded recycled glass aggregates.

2. Materials and methods

2.1. Materials

Seven geopolymeric mortar formulations were developed for this study. In all mixes, fly ash served as the principal aluminosilicate precursor, comprising 90 % of the total precursor mass, and metakaolin was added in a minor proportion to enhance reactivity and contribute to the overall geopolymerization process. Class F fly ash (FA) generated in a coal-fired power plant located in Italy (General Admixture S.p.A.) and MetaStar®501metakaolin from Imerys Minerals Ltd. were used. The chemical compositions of the precursors given by the producers were verified by SEM-EDS analysis, together with the loss of ignition (LOI) values for both fly ash and metakaolin (Table 1).

The alkali-activating solution was prepared by mixing a sodium silicate (SS) solution (Extra Pure by Merck KGaA) with a sodium hydroxide (SH) solution. The sodium hydroxide solution was prepared at a 12-molar concentration by dissolving sodium hydroxide pellets in distilled water. The weight ratio SS/SH was maintained at 2.5.

Lightweight aggregates employed in the study were commercially available (by Poraver) and made of expanded recycled waste glass particles. Five different grain sizes were used (0.04–0.125 mm, 0.1–0.3 mm, 0.25–0.5 mm, 0.5–1 mm, 1–2 mm) and graded according to Fuller's distribution to ensure optimal packing density. The properties of the LWA as provided by the manufacturer are summarized in Table 2.

2.2. Mixing proportions

The reference mix (GPA) was designed based on a formulation previously proposed in the literature [35,36]. An aggregate to the binder (a/b) volume ratio equal to 1.0 was adopted. The amount of alkaline

Table 1
Fly ash and metakaolin compositions obtained by SEM-EDS*.

	Oxides concentration %									LOI %
	SiO_2	CaO	Al_2O_3	Fe_2O_3	K_2O	TiO_2	SO_3	Na_2O	MgO	
Fly ash	59.54	1.76	27.26	2.91	2.71	0.59	1.02	2.56	1.65	3.20
Metakaolin	56.50	2.51	27.92	0.77	1.83	0.44	0.29	9.03	0.71	1.29

*Details on the SEM-EDS analysis are reported in the "2.4 Test Method" section.

Table 2
Properties of expanded waste glass aggregates as declared by the producer.

Properties	Grain Size (mm)				
	0.04–0.125	0.1–0.3	0.25–0.5	0.5–0.1	1–2
Apparent density (kg/m^3)	On req.	850	680	450	410
Dry loose bulk density (kg/m^3)	530	400	340	270	230
Water absorption by mass (%)	On req.	35	28	20	20
Compressive strength (MPa)	On req.	2.8	2.6	2	1.6

activating solution AAS was adjusted to achieve a target flow diameter of 190 mm [37], resulting in a solution-to-binder (s/b) volume ratio of 0.62. In the GPA mix, the aggregates were employed at ambient conditions (dry state), and no extra water was added during mixing.

Three formulations were developed (GPA25, GPA40, and GPA60) to investigate the effect of the saturation grade of aggregates on the final properties of the mortars. The expanded waste glass aggregates were added pre-wetted with different amounts of water. They had a water content of 25, 40, and 60 percent of their weight. These percentages were determined based on technical datasheet information and preliminary laboratory tests. The aggregate supplier furnished the water absorption of each aggregate fraction to reach a saturated surface dry condition (SSD) (Table 2). Considering the amounts of each fraction given by Fuller's distribution, a water absorption of about 25 % of the total weight of aggregates was calculated. On the other hand, laboratory measurements indicated that the water absorbed by SSD aggregates was equal to 60 % of their total weight. The differences with the datasheet were attributed to the difficulties of obtaining a dry surface of the saturated aggregate of finer fractions [35]. The values of 25 % and 60 % and an intermediate water content of 40 % were chosen to prewet the aggregates, and the corresponding GPA25, GPA60, and GPA40 were formulated. Each mix maintained the same a/b as GPA, while the AAS content was adjusted to match the reference workability (190 mm). The resulting s/b values were 0.46, 0.37, and 0.31 for GPA25, GPA40, and GPA60, respectively.

The mix GPA2 was formulated to investigate the effect of the volume of aggregates on the mortar properties. In this formulation, the a/b was increased to 1.5 with the aggregates added in a dry state at ambient conditions. The quantity of alkaline activating solution was adjusted to achieve the same target workability of the reference mix (GPA). This resulted in an s/b value of 0.77.

The GPA3 and GPA3_25 mixes were formulated to investigate the effects of the finest fractions of aggregates. Indeed, the 0.04–0.125 mm, 0.1–0.3 mm fractions were excluded, while only coarser fractions, 0.25–0.5 mm, 0.5–1 mm, 1–2 mm, were employed. The aggregate distribution followed the model of Andreasen and Andersen (A&A) [33,34,38] with the distribution modulus q set to 0.25. This value was selected because the A&A model with q = 0.25 applied to the five fractions of aggregates of GPA resembled Fuller's distribution adopted in the reference mix. GPA3 and GPA3_25 differed for aggregate saturation grades. In GPA3_25, the aggregates were prewetted with an amount of water of 25 % of their total weight, while in GPA3, they were used under ambient conditions. The AAS content of the two mixes was adjusted to achieve the same target workability as the GPA mix. The resulting s/b ratios were 0.59 and 0.43 for GPA3 and GPA3_25, respectively.

The mix proportions of the seven mixes are listed in Table 3. The chosen nomenclature can be summarized as follows:

- GPA was the reference mix with a fixed content and gradation of aggregates. Aggregates were in dry conditions.
- GPA2 and GPA3 corresponded to the mixes in which one of the aggregate parameters of GPA was changed, namely, the aggregate content (suffix 2) and the absence of fines (suffix 3), respectively. Aggregates were in dry conditions.
- GPA25, GPA40, and GPA60 have the same content and gradation of GPA, but aggregates were prewetted with water content of 25 %, 40 %, and 60 % of their weight, respectively.
- GPA3_25 had the same aggregate content and gradation as GPA 3, but aggregates were pre-wetted with a water content of 25 % of their weight.

2.3. Mixing and curing

The mixing procedure followed [35]. The AAS was prepared 24 h before mixing. The dry precursors were mixed in a Hobart mixer at 140 rpm for one minute. The alkaline activating solution was added gradually to dry precursors. After the solution had been added, the mixer continued to work for another five minutes at the same speed. The lightweight aggregates were then added. They were in ambient conditions for GPA, GPA2, and GPA3, while they were prewetted one hour before mixing in the case of the other mixes. After adding aggregates, the mixer ran for another five minutes. The mortars were cast into molds and placed on a shaking table to ensure the homogeneity of the mixture. Specimens were demolded after two to five days, depending on their composition, and then cured under laboratory conditions (23°C, 50 % RH).

2.4. Test methods

The weight of each specimen was monitored during curing up to 40 days from casting. It was determined on five specimens, 40x40x160 mm, for each mix. The bulk density of each specimen was calculated as the ratio of the weight of the specimens at the fortieth day divided by the volume. The last was determined by measuring the dimensions of each side of the specimens at four different points using a caliper.

Porosity accessible to water was evaluated using saturation and

Table 3
Mix proportioning of the geopolymeric mortars. FA: Fly ash; MK: metakaolin; SS: sodium silicate solution; SH: sodium hydroxide solution; EWGA: expanded waste glass aggregates; W: water in the aggregates.

Mix nomenclature	FA+MK (kg/m^3)	SS+SH (kg/m^3)	EWGA (kg/m^3)	W (kg/m^3)
GPA	494.22	305.93	220.56	0
GPA25	524.88	242.71	234.24	59.00
GPA40	545.05	201.13	243.24	97.30
GPA60	558.62	173.13	249.30	150.00
GPA2	408.67	313.62	253.31	0
GPA3	498.65	296.72	190.60	0
GPA3_25	511.36	221.66	195.46	49.00

buoyancy techniques [39]. Three specimens, weighing approximately 20–25 g, were analyzed for each mix. Porosity accessible (P) to water was calculated using the following equation:

$$P = \frac{M_{sat} - M_d}{M_{sat} - M_{sub}} \quad (1)$$

where M_{sat} is the weight of the saturated specimen, M_d is the weight of the dry specimen, and M_{sub} is the saturated submerged weight.

Ultrasonic pulse velocity (UPV) measurements were carried out in direct transmission mode using 150 kHz transducers (Pundit PL 200). The wavelength of the 150 kHz signal was four times the minimum lateral dimension of the specimen and five times the maximum aggregate size, thus respecting the requirements for a correct measurement procedure [40,41]. By repeating the UPV measurements more times at the same point, a velocity error of 0.3 % was estimated, obtained by combining the relative errors of time and thickness measurements. Four measurements along the 40 × 160 mm faces were considered, and the average value was calculated for each specimen. UPVs were assessed on the same specimens and at the same times as those used for weight monitoring.

After 40 days from casting, all the 40x40x160mm specimens were tested to estimate flexural and compressive strength [42]. The results of each mechanical property were obtained by averaging the results of five specimens per mix.

The thermal conductivity of the mortars was measured on disk-like specimens, 50 mm in diameter (FOX 50 Laser Comp - TA Instruments) according to [43,44]. The two-thickness method was used, as it provides the highest precision available for the instrument (3 %) and allows the estimation of the thermal conductivity of the specimen and the contact thermal resistance. The two thicknesses were 15 mm and 6 mm. Specimen surfaces were lapped to minimize the roughness and ensure good contact with the instrument plates. The upper plate temperature was set to 15°C and the lower plate to 25°C. Two couples of specimens were tested for each batch, and the average value was calculated. The specimens were tested after 40 days, in oven-dry conditions (oven-dried at 60°C until a constant weight was reached).

Morphological analysis of the mortars was performed by scanning electron microscope (SEM ZEISS EVO 15) equipped with Energy Dispersive X-ray Spectrometer (EDS) (Oxford Instruments) and tungsten filament. The specimens analyzed were fragments collected from the broken samples after compressive strength testing. The SEM analysis was performed using secondary electrons in low-vacuum mode on samples without metallization. The operation conditions were as follows: working distance 10 mm, accelerating voltage 25 kV, variable pressure 90 Pa, scan speed 9, and cycle time 23 s. AZtec 6.0 SP1 software platform and an Ultim MAX 40 mm^2 SSD detector (Oxford Instruments, Abingdon-on-Thames, UK) with a resolution of 127 eV FWHM @MnKa and a detection limit of about 0.1 wt% from 0.3 to 3 μm in depth, were used for EDS analysis. The software module uses a standardless ZAF quantification system. EDS was used to determine the composition of precursor powders. In this case, the measurement was performed at ten different points among different powder particles, and the mean of the oxide percentage was determined (Table 1).

3. Results

3.1. Aggregate prewetting

The GPA25, GPA40, and GPA60 mixes had aggregates pre-wetted with different amounts of water. Prewetted aggregates absorbed less alkaline solution than dry aggregates during mixing, improving workability. As a result, increasing the water content in the aggregates allowed for a lower AAS content in the mix to achieve the same workability as GPA. This aspect influenced the weight and UPV variations over time (Fig. 1) as well as the final properties of the mortars.

The weight loss was determined by referring to the final weight recorded at forty days. All mixes experienced weight loss during curing due to water evaporation. The weight monitoring evidenced a steeper weight loss in the mixes containing pre-wetted aggregates compared to the GPA mix. This was particularly evident in the first two weeks. After this period, weight variation was negligible in all mixes except GPA, which continued to lose weight at a slower rate (Fig. 1a).

Regarding the UPV variation, as for weight loss results, the final value of 40 days was taken as the reference (Fig. 1b). The behavior of the mixes containing free water in aggregates differed from GPA. The ultrasound velocity of GPA increased gradually until the twelfth day, after which a reduction in ultrasonic velocity was observed. GPA25, GPA40, and GPA60 had UPV values higher than GPA after demolding. Then, the UPV behavior in the first week varied depending on the solution content. In GPA25, the UPV increase was observed until the fifth day, when it reached a velocity value close to the final one. Then UPV decreased until the twelfth day and increased again by 15 %. In GPA40, ultrasound velocity decreased after demolding and continued until the seventh day. Then, a continuous increase in UPV of 25 % was observed. In GPA60, UPV behavior resembled GPA40. The UPV increase was 34 % and started on the sixth day. Both the mixes had a constant value of UPV after twenty days.

SEM analysis gave information about the morphology of the different mixes, contributing to a better understanding of the geopolymerization reaction results. The GPA mix showed a uniform morphology, where unreacted and partially reacted fly ash particles were identifiable (Fig. 2a) within the geopolymeric matrix. The GPA25 mix showed a lumpy morphology with unreacted fly ash particles (Fig. 2b). In contrast, the GPA40 mix displayed uniform and compact morphology, with

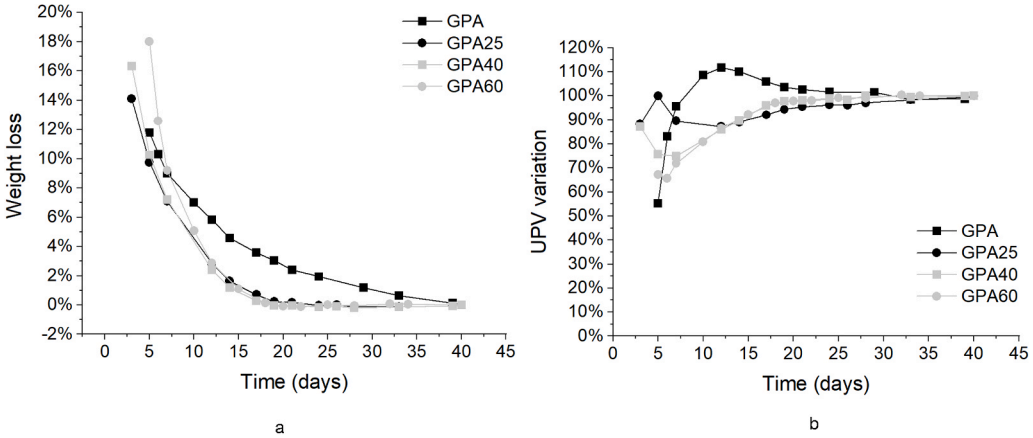

Fig. 1. Weight loss (a) and UPV variation (b) with time for GPA; GPA25, GPA40, and GPA60 mortars.

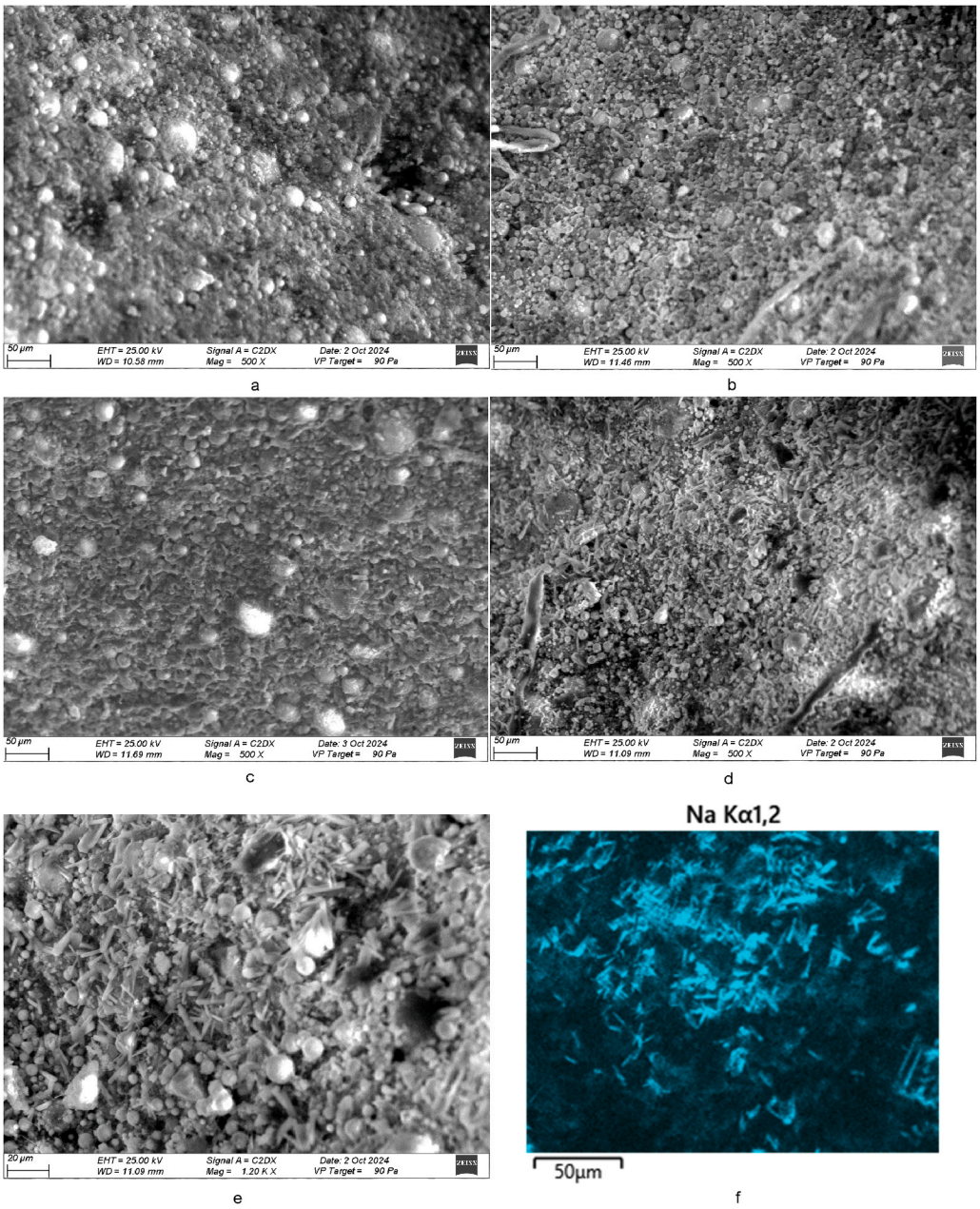

Fig. 2. SEM images of a) GPA, b) GPA25, c) GPA40, d) GPA60, e) efflorescence in GPA60. f) EDS map of sodium in GPA60 mortar.

significantly fewer unreacted particles than in the previous two mixes (Fig. 2c). The GPA60 mix had a discontinuous, porous morphology with numerous unreacted fly ash particles and needle-like salt efflorescence. The latter are evidenced by the sodium maps obtained through EDS analysis (Fig. 2e, f).

The degree of aggregate saturation and the consequent content of alkaline activating solution in the mixes influenced their physical properties (Fig. 3). The GPA mix had the highest density and thermal conductivity, with the lowest porosity. The opposite was for GPA60, following SEM results. Indeed, the thermal conductivity is proportional to density and inversely related to porosity. The observed differences were caused by the higher amount of alkaline solution in GPA compared to the other mixes, since AAS had a higher density than the water present in GPA25, GPA40, and GPA60.

The GPA, GPA25, and GPA40 had comparable compressive strengths (Fig. 4a). The GPA25 mix had slightly lower flexural strength than GPA and GPA40, and a lower UPV value (Fig. 4b). Thus, it can be observed that GPA40 had the best compromise between mechanical strengths (comparable to GPA), high ultrasonic velocity, and low density and thermal conductivity.

3.2. *Increase in the aggregate content*

The mix GPA2 had higher aggregate-to-binder and solution-to-binder ratios than GPA. The latter was necessary due to the increased aggregate content compared to GPA, which led to greater absorption of the alkaline solution. The performance of GPA2 was evaluated against GPA to investigate the influence of aggregate content on the mortar's properties. Despite the higher alkaline solution content, the weight variation over time for GPA2 was comparable to that of the GPA mix (Fig. 5a). Both mixtures continued to lose weight over the 40-day monitoring period. The evolution of UPV differed between the two mixes: GPA2 showed a lower increase than GPA (Fig. 5b). In GPA2, the decrease in UPV observed in GPA was not apparent, and UPV values

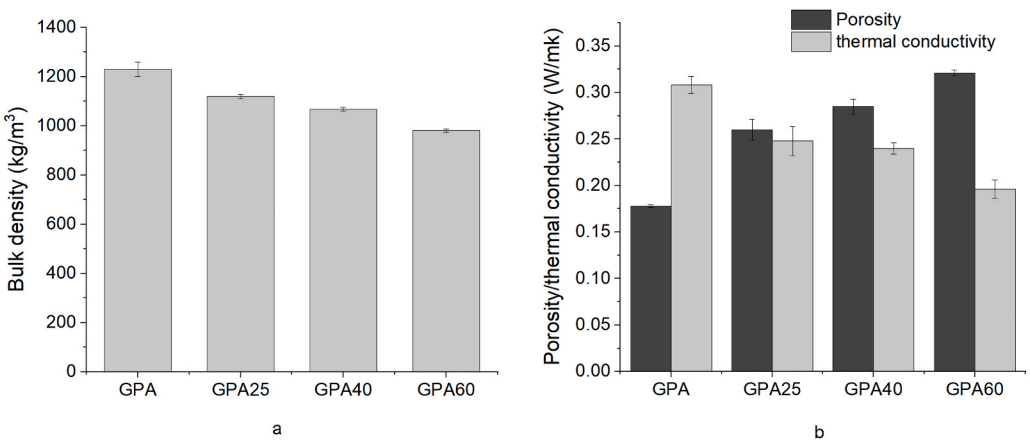

Fig. 3. Physical properties of the mortars: a) bulk density, b) Porosity/thermal conductivity.

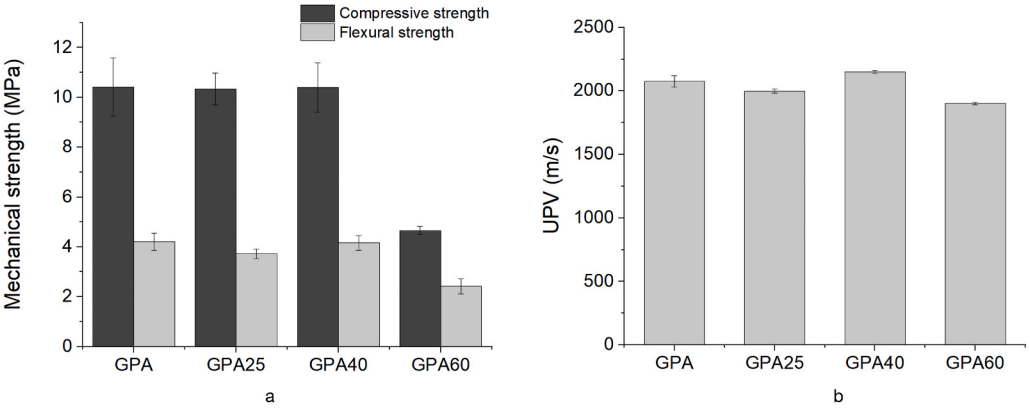

Fig. 4. Compressive/flexural strengths (a), and ultrasonic pulse velocity (b) of the mortars.

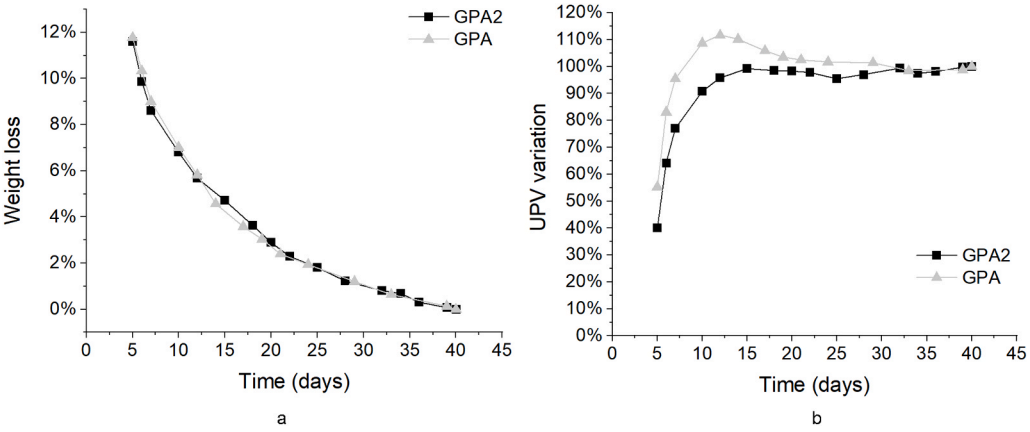

Fig. 5. Weight loss (a) and UPV variation (b) with time for GPA and GPA2 mortars.

stabilized approximately two weeks after casting, remaining nearly unchanged up to 40 days.

The SEM analysis showed that the GPA2 morphology was compact and dense (Fig. 6a). The unreacted fly ash particles were fewer than in GPA (Fig. 6b) and well encapsulated in the geopolymer matrix. Few voids and microcracks were visible.

GPA2 had a bulk density comparable to GPA (Fig. 7a). Indeed, the lightening effect induced by aggregate volume was offset by the higher amount of the alkaline solution, which contributed to an increase in density. The greater aggregate volume led to a reduction in thermal conductivity without affecting the water-accessible porosity (Fig. 7b). The mechanical properties and UPV values of GPA2 were slightly higher than those of GPA (Fig. 7c, d), reflecting the morphological properties of the two materials.

3.3. *Absence of fine aggregates*

The fine aggregates strongly influenced the weight and UPV changes over time (Fig. 8). The weight variation of GPA3 and GPA3_25 followed a comparable trend (Fig. 8a), however, this similar trend was not

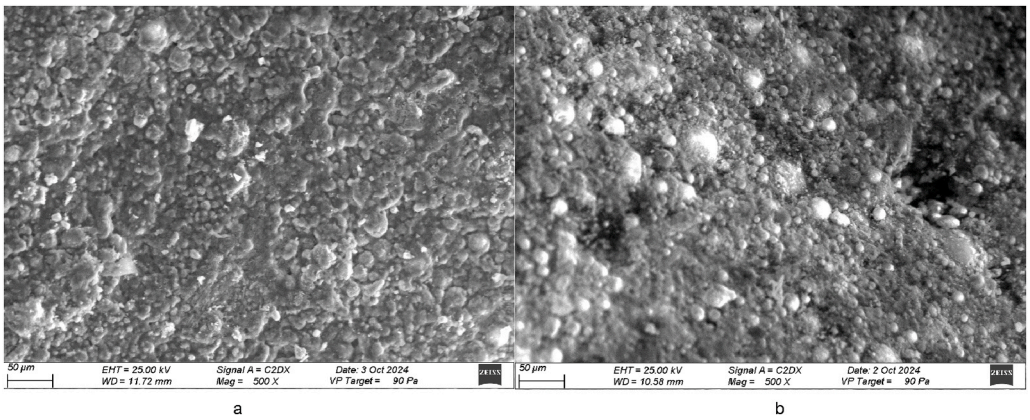

Fig. 6. SEM images of GPA2 (a) and GPA (b).

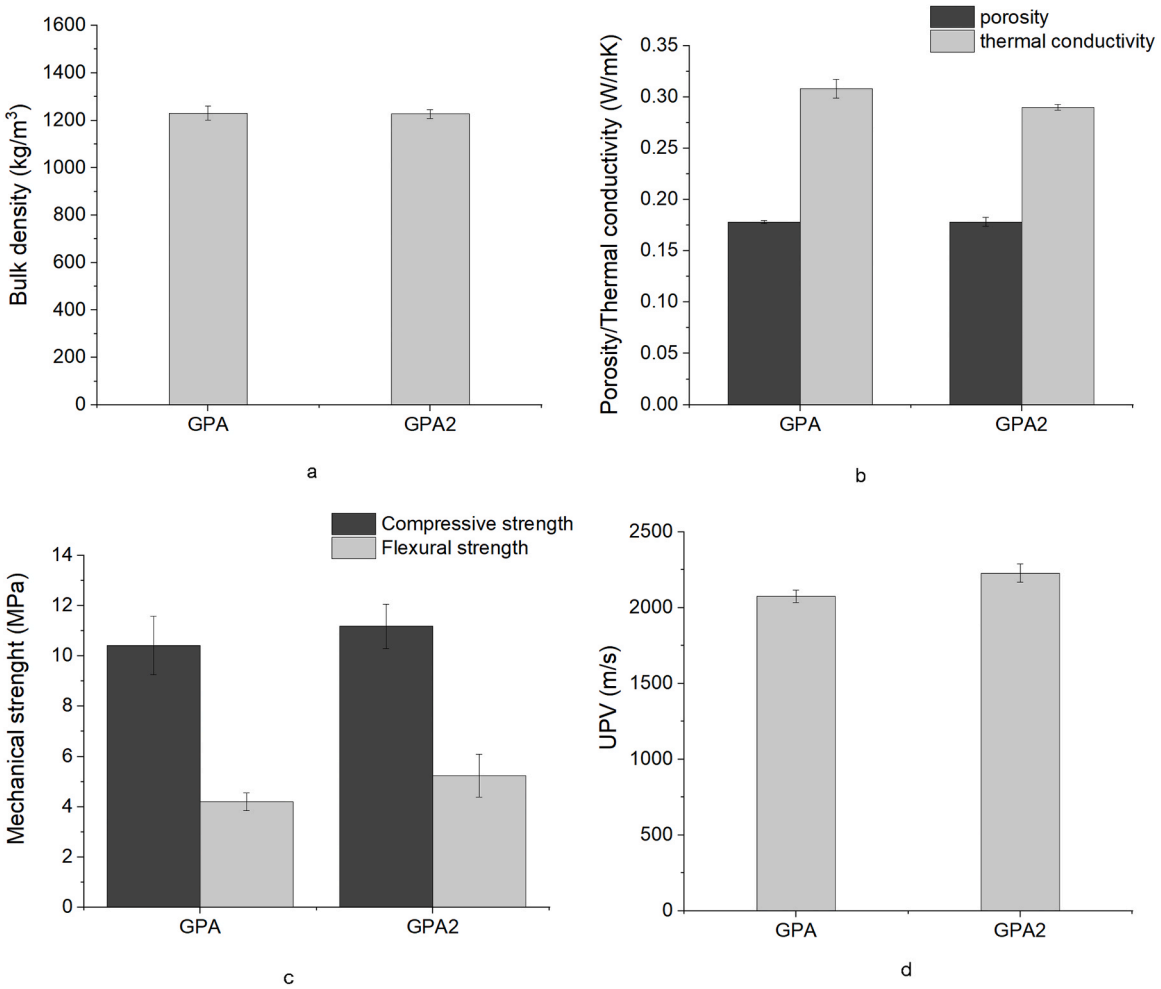

Fig. 7. Physical and mechanical properties of GPA2 and GPA mortars: a) bulk density, b) Porosity/thermal conductivity, c) compressive/flexural strength, d) UPV.

observed comparing the GPA mix and the GPA25 mix. In the latter case, the additional water retained by the aggregates led to markedly different behaviors. Notably, the mixture containing fine aggregates exhibited a more substantial total weight loss, despite having the same initial solution and water content as the GPA3 and GPA3_25 mixtures. In contrast, the weight loss in the mixes without fine aggregates occurred primarily during the first week in a rapid manner, then slowed until the twelfth day and became negligible by the twentieth day.

Comparing UPV results of GPA3 and GPA, the gradual increase of UPV in GPA until the twelfth day was absent in GPA3, which ended the ultrasound velocity increase as early as the fourth day (Fig. 8b). This was followed by a gradual decline of ultrasound velocity until the fourteenth day, after which a 5 % increase was recorded. In the GPA3_25 mixture, ultrasound velocity exhibited a rapid increase during the first three days, followed by a decrease. Subsequently, an additional 10 % increase in UPV was observed after two weeks.

The SEM image of the GPA3 mix showed an inhomogeneous microstructure with several unreacted fly ash particles and voids

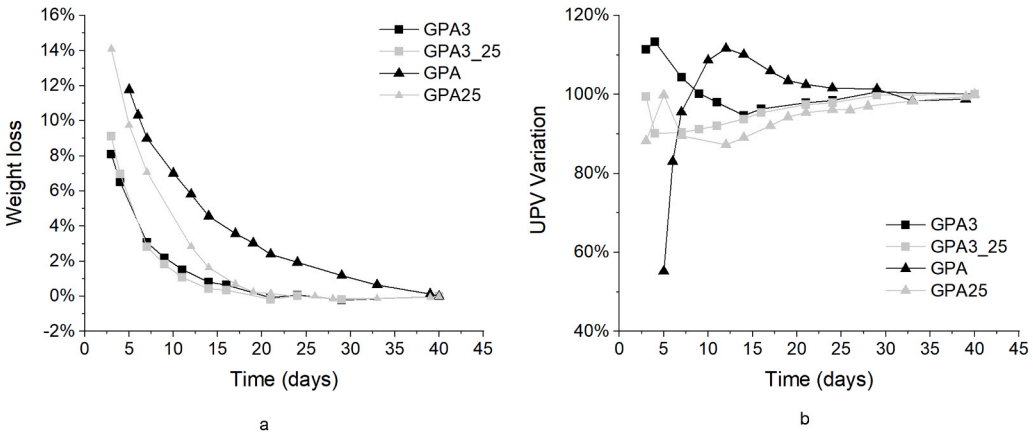

Fig. 8. Weight loss (a) and UPV variation (b) with time for GPA 3, GPA3_25, GPA, and GPA25 mortars.

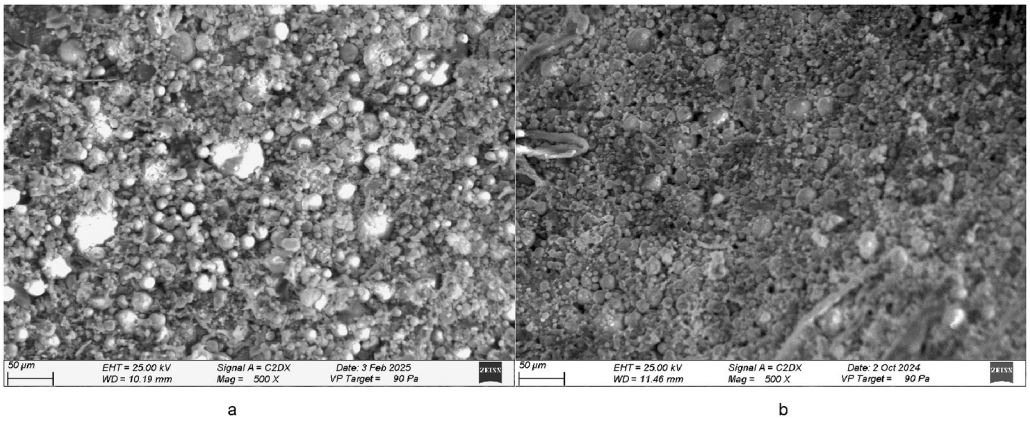

Fig. 9. SEM images of GPA3 (a) and GPA3_25 (b).

(Fig. 9a). The GPA3_25 mix had more geopolymer gel and fewer unreacted fly ash particles (Fig. 9b). On the other hand, microcracks and accumulation zones of the unreacted particles not linked by geopolymer gel were observed.

The bulk densities and thermal conductivity of GPA3 and GPA3_25 mixes were lower than those of GPA and GPA 25, respectively (Fig. 10). This was due to the finest fraction substitution with coarser aggregates of lower density. The porosity of GPA3 and GPA3_25 mixes was higher than that of GPA and GPA25, respectively (Fig. 10b). The results followed those of morphological analysis, which evidenced a cracked and porous microstructure.

The compressive and flexural strength of the GPA3 and GPA3_25 mixes were lower than the corresponding mix with fines (Fig. 11a). The UPV values were consistent with the results of the other physical and mechanical tests, showing lower UPV values in the absence of fines (Fig. 11b). GPA3_25 mix had better mechanical performance than GPA3, probably due to a higher degree of geopolymerization reactions.

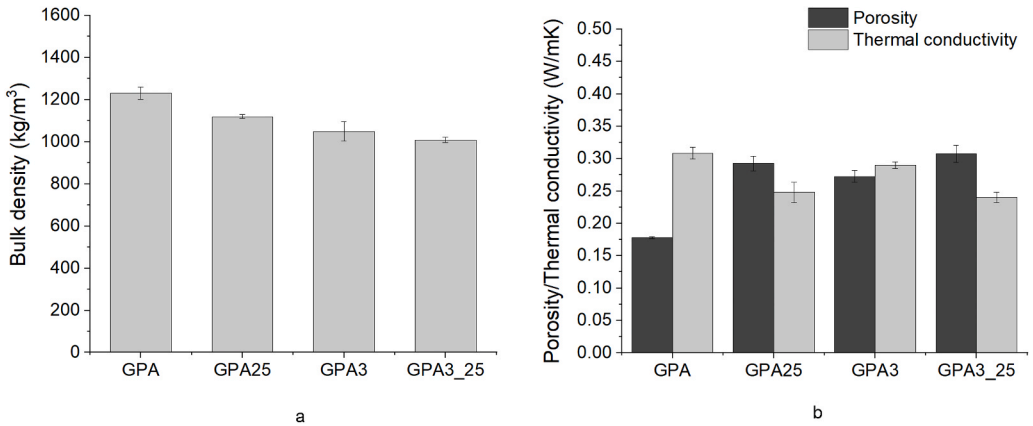

Fig. 10. Physical properties of GPA, GPA25, GPA3, and GPA3_25 mortars: bulk density (a) and Porosity/thermal conductivity (W/mk).

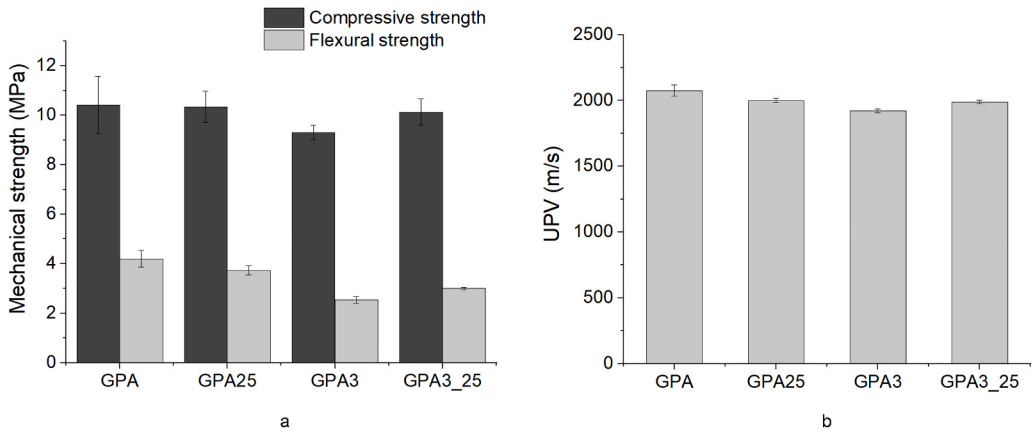

Fig. 11. Mechanical properties of GPA, GPA25, GPA3, and GPA3_25 mortars: Compressive/flexural strength (a) and UPV (b).

4. Discussion of results

4.1. Weight and UPV monitoring

All the mortars investigated exhibited weight loss over time, with different trends depending on the mix composition (Fig. 12). The observed weight loss was primarily attributed to the evaporation of water from the mix. During geopolymerization reactions, water acts as the medium, and it participates in several intermediate reactions, such as dissolution, polycondensation, etc. In the final stage of the reaction, water molecules become reaction products and are subsequently released [45,46]. The mixes displayed different rates of water loss during curing, resulting in varying degrees of weight loss. Notably, when the finest fractions were absent from the mix, the weight loss was more pronounced after demolding, with nearly all the weight loss occurring within twenty days (Fig. 12). Conversely, GPA and GPA2 exhibit a more gradual water loss throughout the monitoring period. The presence of water within aggregates had the same effect as the absence of fines. Indeed, a steeper weight reduction was observed after demolding for up to two weeks in mixes containing higher water content within the aggregates, namely GPA60 and GPA40, followed by GPA25 and GPA3_25 (Fig. 12b). It can be hypothesized that in GPA3 and GPA3_25, the absence of fines allowed for more efficient water evaporation before demolding compared to the other mixes. Indeed, the total weight loss in GPA3 and GPA3_25 ranged between 8 % and 9 % in contrast to 12–14 % in GPA and GPA25, despite having comparable liquid content in the mix.

To better understand the weight loss behavior of the mortars, the UPV trend was deeply analyzed. According to literature, UPV in geopolymers generally increases over time as a result of ongoing geopolymerization reactions [47,48]. In the present study, UPV measurements were performed multiple times after demolding, evidencing different trends for which no comparable studies are currently available in the literature. The observed UPV behavior over time can be attributed to the simultaneous influence of two phenomena during the curing process: i) weight loss due to water evaporation; ii) material hardening due to the progression of the geopolymerization reactions. Water evaporation leads to the replacement of water with air in the material pores, thereby reducing UPV. In contrast, material hardening increases UPV as the matrix becomes denser and more rigid. The result of the UPV trend reflects the balance between these two opposing effects, with the prevalence of one determining the trend of UPV measurements [35]. The analysis of UPV trends across different mortar compositions allowed valuable insights into the role of alkaline solution absorption by aggregates in influencing the rate and extent of geopolymerization progress. This understanding is critical for material application on-site, as it helps to determine the time required for the material to develop adequate mechanical performance.

The role of fine aggregates was crucial in UPV development (Fig. 13a). The geopolymerization progress was indicated by an increase in UPV in the first days after demolding. In the GPA mortar, the geopolymerization process progressed more slowly and gradually compared to the GPA3 mix, with a total duration of approximately twelve days. The GPA2 mixture, which contained a higher proportion of fine aggregates due to the higher volume of EWGA, exhibited an even slower reaction, with geopolymerization extending for about two weeks. In GPA3, geopolymerization can be considered almost concluded after four days. Furthermore, it was not possible to demold GPA and GPA2 specimens before the fifth day, as the geopolymerization process was still at an early stage. Premature removal of the molds would lead to spalling of the specimens under their own weight due to the high density of alkaline

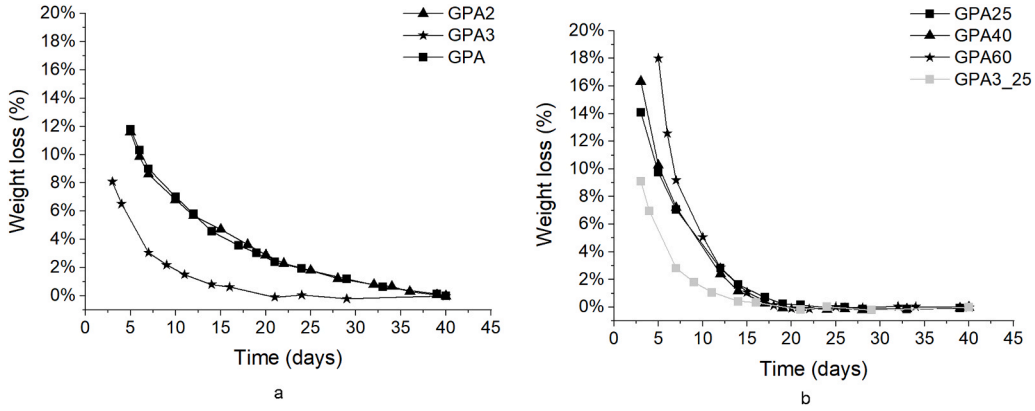

Fig. 12. Weight loss of the mixes in the case of dry aggregates (a) and prewetted aggregates (b).

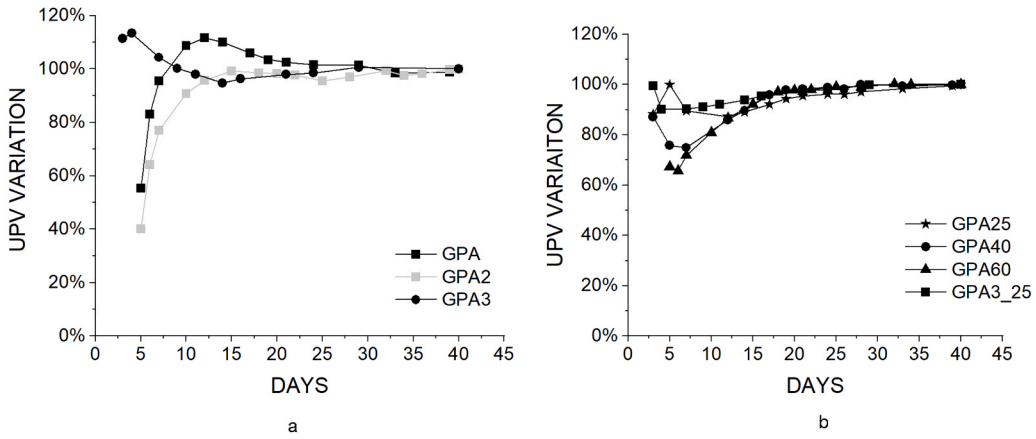

Fig. 13. UPV variation of the mixes in the case of dry aggregates (a) and prewetted aggregates (b).

solutions. In contrast, demolding of GPA3 was possible the day after the casting of the specimens. The primary differences between GPA3 and the other mixes were due to the greater absorption of AAS by fine aggregates compared to coarser ones. In GPA and GPA2, fine aggregates absorbed a significant amount of AAS during mixing, forming a sludge in which the precursor particles were dispersed. This absorbed solution was released gradually, thereby delaying the onset of effective geopolymerization, which became evident only after five days.

The subsequent phase, characterized by a reduction of UPV due to water evaporation, also varied among the three mixes. In GPA3, this phase was rapid and ended in two weeks, while it continued from twelve to thirty days in GPA. In GPA2, the effect was negligible. The rapid geopolymerization of GPA3 caused an excess of water; hence, following demolding, water evaporation dominated over matrix hardening, which was nearly complete. This caused a noticeable decrease in UPV. In GPA, the longer duration of geopolymerization allowed a more gradual water loss, resulting in a moderate reduction in UPV. In GPA2, a balance was achieved between material hardening and water loss, resulting in a relatively stable UPV value throughout the monitoring period.

As observed in the absence of the fine portion of aggregates, a higher reaction rate in the initial curing phase was also observed in the mix incorporating pre-wetted aggregates (Fig. 15b). In these mixes, the pre-saturation of the fine aggregates prevented the formation of the sludge, which is responsible for delaying the reaction process. Consequently, the early stages of reaction progressed more rapidly, as reflected by higher UPV values recorded on the fifth day compared to the GPA mix. Indeed, all the mortars with prewetted aggregates achieved UPV values higher than about 70 % of their final value within the first five days, in contrast with GPA and GPA2, which developed only 55 % and 40 % of their respective UPV final value over the same period. Furthermore, it was possible to demold all the specimens with prewetted aggregates before the fifth day without damage. In the GPA60 and GPA40 mixes, a sudden reduction in ultrasound was observed immediately after demolding, attributed to rapid water evaporation. This initial decrease was followed by a progressive increase in UPV, corresponding to continued geopolymerization, until values stabilized. Different behaviors were observed in GPA3_25 and GPA25. The higher content of AAS in these mixes led to a more advanced stage of geopolymerization within the first week. Specifically, the process was nearly complete after five days in GPA25 and after three days for GPA3_25. In the case of GPA25, the presence of fine aggregates, which were probably not fully saturated, resulted in a partial AAS absorption, which slowed the geopolimerization compared to GPA3_25.

4.2. Final properties of the mortars

The EWGA parameters influenced both the geopolymerization process and the final properties of the mortars. Variation in the AAS contents across the mixes varied the Si/Al, Na/Al molar ratios, as well as the water/binder (w/b) weight ratio, due to changes in the proportions between the free water and the water contained within the alkali solution. According to the literature, Na/Al, Si/Al, and w/b ratios are the main parameters affecting the final performance of the geopolymer materials [26,46,49,50]. Generally, a more alkaline environment with high values of Na/Al and Si/Al enhances mechanical properties up to an optimum value beyond which further increases can lead to a decline in performance. Conversely, an increase in the w/b ratio tends to reduce mechanical strength once the minimum w/b value is required to have good workability. These results were observed in geopolymers with normal-weight aggregates.

The experimental results showed no clear trend between the material's mechanical properties and the studied ratios (Fig. 14). This behavior can be attributed to the use of EWGA, which are lightweight aggregates. When not fully saturated, these aggregates absorbed part of the AAS during mixing. As a result, the amount of AAS in direct contact with the binder varied based on the aggregate's absorption and subsequent release of the solution over time during curing. Therefore, in the mortars investigated, the content of the alkaline solution was not directly proportional to mechanical strength.

The compressive strengths of the GPA, GPA25, GPA40, and GPA3_25 mortars were comparable (Fig. 15), all measuring around 10 MPa. Notably, the flexural strengths of GPA, GPA25, and GPA40 also exhibited similar values (Fig. 15). These results indicated that reducing the alkaline solution content by prewetting aggregates did not affect the mechanical performance of the mixes. On the other hand, a threshold in AAS content under which the mechanical performances deteriorate was identified, as demonstrated by the results of the GPA60 mix. In this case, the compressive and flexural strengths of GPA60 were 55 % and 42 % lower, respectively, than GPA. The reduced strength in the GPA60 is attributed to an insufficient amount of alkaline solution to complete the geopolymerization process. This is further supported by the presence of efflorescence observed in SEM analysis (Fig. 2e, f), which typically forms when there is an excess of alkaline solution or when the geopolymerization reactions are incomplete [51].

The compressive strengths of GPA2 and GPA3 were slightly higher (7 %) and slightly lower (10 %) than GPA, respectively (Fig. 15). These differences were due to the aggregate grading and content.

In GPA2, the increase in the aggregate-to-binder volume ratio caused a higher solution-to-binder ratio and higher mechanical performance than GPA (Fig. 15). The increase in the aggregate content did not worsen the mechanical properties as reported in the literature for concrete [52–55]. It was probably due to the better adhesion between glass aggregates and geopolymeric binder than in OPC, according to literature results [23,56,57].

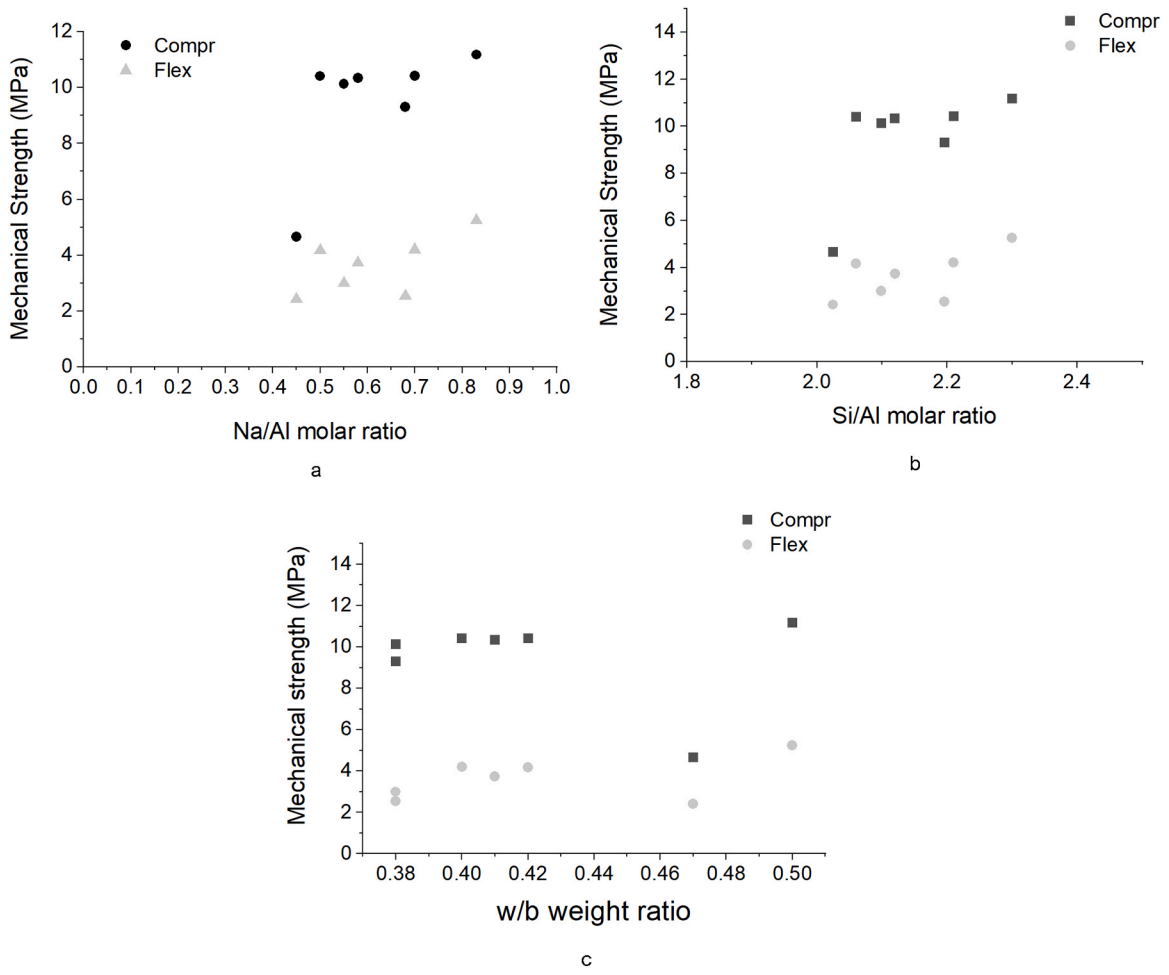

Fig. 14. Mechanical strength variation with Na/Al molar ratio (a), Si/Al molar ratio (b), w/b weight ratio (c).

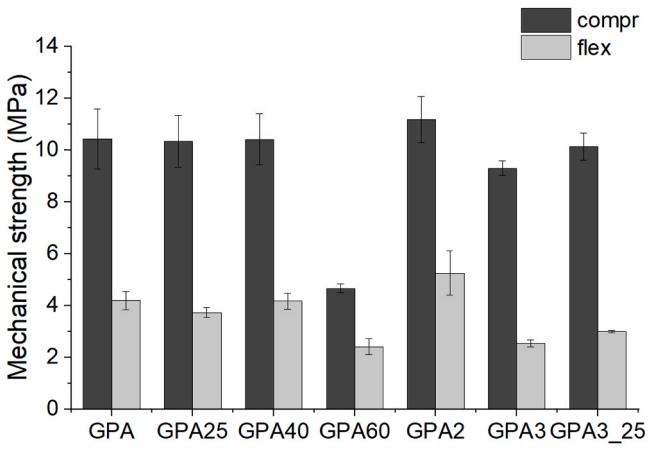

Fig. 15. Mechanical strengths (compressive /flexural strengths) of the mortars.

In contrast, the lack of fines in GPA3 resulted in reduced compressive and flexural strength compared to GPA. GPA3_25 mix showed a reduction in flexural strength but maintained compressive strength similar to GPA. The flexural behavior is associated with the presence of voids and micro-cracking in the geopolymeric matrix as confirmed by SEM analysis (Fig. 9). The positive role of fine glass aggregates in reducing microcracking and enhancing mechanical properties was also found in the literature for both OPC and geopolymers concretes [23,33,58,59]. Fines caused cracks to travel longer distances to overcome aggregates, requiring more energy, and resulting in greater mechanical strength. Furthermore, the literature hypothesized that the fine particles exhibit pozzolanic activity in OPC concrete and may also contribute to the geopolymerization reactions due to partial silica dissolution from the fine glass aggregates [58].

The compressive strength of GPA3_25 was higher than GPA3, probably due to higher geopolymerization progress, as supported by SEM observation. The lower AAS absorption by coarse aggregates caused an excess in the alkaline solution in GPA3 compared to GPA, which may have hindered the progression of geopolymerization reactions [60]. In GPA3_25, the AAS content was lower than GPA3, facilitating the progress of geopolymerization.

Flexural strengths reflected, more than compressive strength, the variations in microstructure as revealed by SEM analysis (Fig. 15). As discussed previously, GPA3 and GPA3_25 exhibited lower flexural strength due to the micro-cracking of the geopolymeric matrix. Their flexural strength values were comparable to that of GPA60, which also showed voids and an inhomogeneous morphology. In contrast, GPA2 exhibited a 25 % increase in flexural strength compared to GPA, consistent with its more homogeneous matrix and the absence of voids and microcracks in SEM images. On the contrary, the flexural strength of GPA25 was 11 % lower than GPA, reflecting the lumpy morphology of the geopolymeric matrix. The flexural strength results showed a strong correlation with UPV values at the end of the monitoring period (Fig. 16a), in agreement with the microstructural characteristics of the materials. On the other hand, excluding the values of GPA60, the correlation of compressive strength with UPV improved, yielding a coefficient of determination of 0.8.

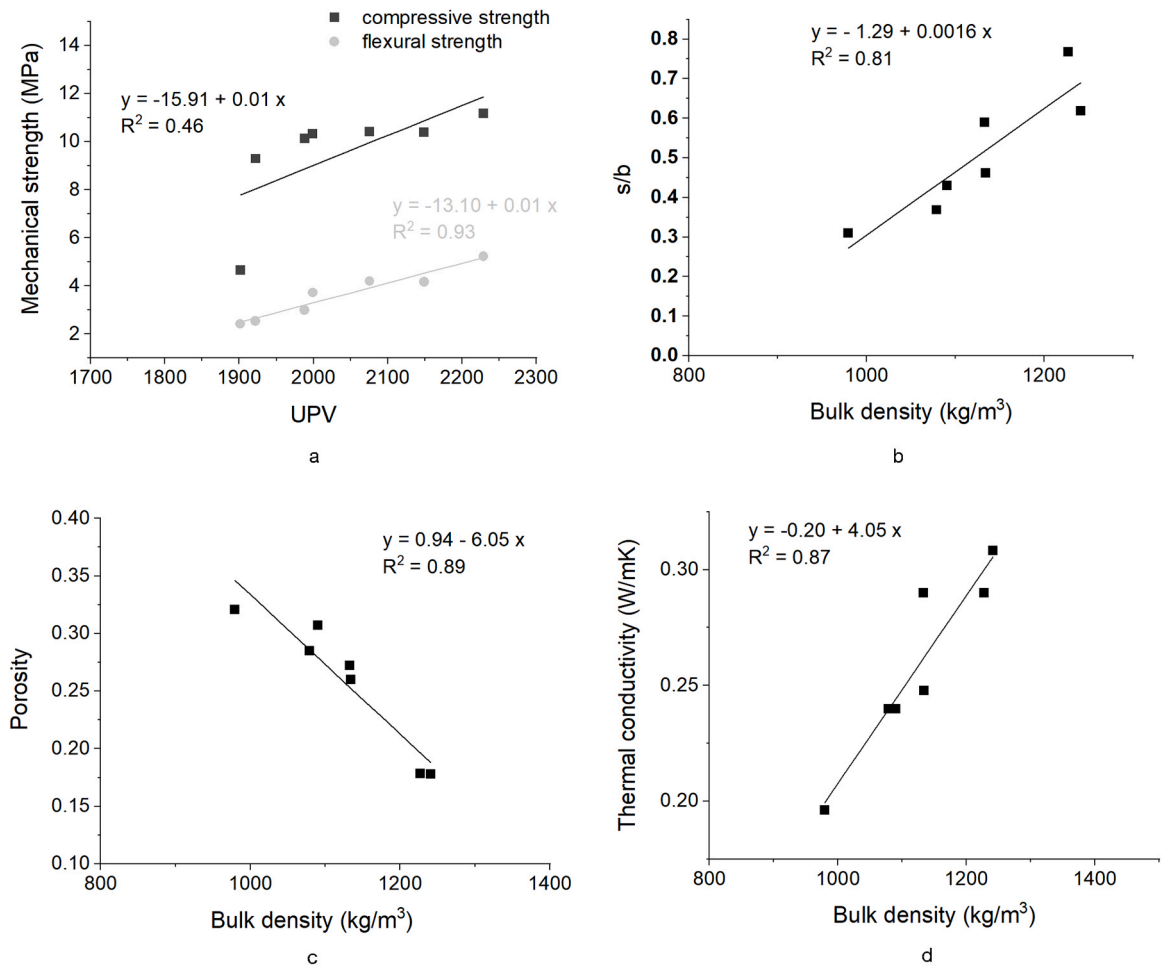

Fig. 16. Linear correlations between: mechanical strength (compressive/flexural) and UPV (a); s/b and bulk density (b); porosity and bulk density (c); thermal conductivity and bulk density (d).

Unlike mechanical properties, the physical properties of the mortars were influenced by the content of AAS added during mixing (Fig. 16). Increasing the alkaline solution-to-binder ratio led to an increase in the bulk density (Fig. 16b), which in turn was strongly correlated with both porosity and thermal conductivity (Fig. 16c, d). In particular, when the content of the alkaline solution was higher, it resulted in lower porosity and higher density and thermal conductivity.

5. Conclusions

This study investigated the effect of saturation grade, amount, and grading of expanded waste glass aggregates (EWGA) on the physical/mechanical properties of geopolymeric mortars. EWGA, as lightweight aggregates, are characterized by higher porosity compared to conventional aggregates, leading to increased liquid absorption during mixing. The analyzed EWGA parameters strongly affected this aspect, thereby influencing the geopolymerization process and final properties of the mortars. While several works in the literature deal with these aspects for OPC concrete/mortars, limited research exists regarding their impact on geopolymers. This work aims to contribute to expanding the knowledge of EWGA behavior in geopolymers, with the ultimate scope of promoting the employment in building technology of waste materials, used in both the aggregates and geopolymeric mortar matrix.

Experimental results highlighted the critical role of the fine fraction of EWGA in both the geopolymerization process and final mortar properties. Fine aggregates were primarily responsible for absorbing the alkaline solution during mixing, leading to the formation of a sludge in which the precursor particles were dispersed. This absorption slowed the geopolymerization reaction, making it impossible to demold specimens before five days. On the other hand, the absence of fine aggregates caused the worsening of mechanical properties due to microcracking as revealed by SEM analysis. Additionally, density and thermal conductivity were lower in mixes without fine aggregates, attributable to the comparatively lower density and higher porosity of coarse aggregates.

Prewetting the aggregates prevented the formation of the sludge of fine aggregate particles and the alkaline solution, leading to a faster geopolymerization process. Additionally, prewetting aggregates enabled a reduction in the AAS content in the mortars while maintaining the same mechanical performance as mortars with dry aggregates, thereby lowering density and thermal conductivity. However, a threshold level for AAS reduction was identified, below which mechanical strengths significantly declined. Therefore, prewetting aggregates up to this threshold can preserve mortar performance and simultaneously decrease the amount of silicate solution, which is costly and environmentally impactful [61–63].

The increase in EWGA volume caused an increase in the alkaline solution content to obtain the same workability as the reference mix, slowing geopolimerization reactions. GPA2 exhibited improved mechanical properties compared to GPA, along with reduced thermal conductivity and comparable density. This finding did not follow the literature results for OPC concrete, for which the aggregate volume increase caused a worsening of the mechanical performance. This discrepancy may be attributed to the better adhesion of aggregates with geopolymers than the OPC matrix, as reported in the literature. Further

research is needed to investigate the effect of prewetting aggregates under these conditions.

Another key finding of this study is the demonstrated utility of ultrasonic velocity measurement for monitoring geopolymer curing. UPV effectively tracks the progression of the material's curing reactions and is well correlated with material mechanical properties, particularly flexural strength.

CRediT authorship contribution statement

vasanelli emilia: Writing – review & editing, Writing – original draft, Methodology, Investigation, Formal analysis, Data curation, Conceptualization. **Silvia Calò:** Validation, Methodology, Investigation, Data curation. **Marianovella Leone:** Writing – original draft, Visualization, Validation, Supervision. **Maria Antonietta Aiello:** Validation, Supervision, Resources, Project administration, Funding acquisition.

Declaration of Competing Interest

The authors declare that they have no known competing financial interests or personal relationships that could have appeared to influence the work reported in this paper.

Acknowledgements

The Authors would like to thank Sipre Srl for its valuable support in sample making and workability testing.

Funding

The research presented in this article was funded by the Italian Ministry of University and Research in the framework of the national research project PRIN (Progetti Di Ricercar Di Rilevante Interesse Nazionale – Bando 2022) – Project PRIN sTructurAl and energy rEnovation for sustainable buildingS – TARGETS.

Data availability

Data will be made available on request.

References

[1] A.M. Neville, Properties of concrete, Longman, England, 1995.
[2] S. Chandra, L. Berntsson, Lightweight aggregate concrete science, technology and applications, Delhi India. Stand. Publ. Distrib. (2003).
[3] M.S.T. Masoule, N. Bahrami, M. Karimzadeh, B. Mohasanati, P. Shoaei, F. Ameri, T. Ozbakkaloglu, Lightweight geopolymer concrete: a critical review on the feasibility, mixture design, durability properties, and microstructure, Ceram. Int. 48 (8) (2022) 10347–10371.
[4] M.S. Nasr, A.A. Shubbar, Z.A.A.R. Abed, M.S. Ibrahim, Properties of eco-friendly cement mortar contained recycled materials from different sources, J. Build. Eng. 31 (2020) 101444.
[5] R.S. Rathore, H.S. Chouhan, D. Prakash, Influence of plastic waste on the performance of mortar and concrete: a review, Mater. Today. Proc. 47 (2021) 4708–4711.
[6] R.I. Gomes, C.B. Farinha, R. Veiga, J. de Brito, P. Faria, D. Bastos, CO2 sequestration by construction and demolition waste aggregates and effect on mortars and concrete performance-An overview, Renew. Sustain. Energy Rev. 152 (2021) 111668.
[7] S. Nasier, Utilization of recycled form of concrete, E-wastes, glass, quarry rock dust and waste marble powder as reliable construction materials, Mater. Today. Proc. 45 (2021) 3231–3234.
[8] Q.L. Yu, D.J. Glas, H.J.H. Brouwers, Effects of hydrophobic expanded silicate aggregates on properties of structural lightweight aggregate concrete, J. Mater. Civ. Eng. 32 (6) (2020) 06020006.
[9] S.K. Adhikary, D.K. Ashish, Ž. Rudžionis, Expanded glass as lightweight aggregate in concrete–A review, J. Clean. Prod. 313 (2021) 127848.
[10] H.W. Kua, W.S. Teoh, X. Xu, B. Huang, Y. Geng, A review of glass recycling policies in Stockholm, Hong Kong Sar and shanghai from a circular economy perspective, J. Clean. Prod. 434 (2024) 140068.
[11] Trends in Solid Waste Management. Available online: ⟨https://datatopics.worldbank.org/what-a-waste/trends_in_solid_waste_⟩ management.html (accessed on 14 May 2020).
[12] Glass Packaging Institute ⟨https://www.gpi.org/facts-about-glass-recycling⟩ (accessed May 2025).
[13] V. Ducman, A. Mladenovĭ c, J.S. ˇ Suput, Lightweight aggregate based on waste glass and its alkali-silica reactivity, Cem. Concr. Res. 32 (2002) 223–226, https://doi.org/10.1016/S0008-8846(01)00663-9.
[14] P. Chindaprasirt, T. Cao, F. Pacheco-Torgal, J.A. Labrincha, C. Leonelli, A. Palomo 2015. 19 - Reuse of recycled aggregate in the production of alkali-activated concrete. In: Chindaprasirt Mortars and Concretes, P.B.T.-H. Of A.-A.C. Woodhead Publishing, Oxford, pp. 519–538. https://doi.org/10.1533/9781782422884.4.519..
[15] R.N. Swamy, The Alkali-silica reaction in concrete, CRC Press, 2002.
[16] F. Rajabipour, E. Giannini, C. Dunant, J.H. Ideker, M.D. Thomas, Alkali–silica reaction: current understanding of the reaction mechanisms and the knowledge gaps, Cem. Concr. Res. 76 (2015) 130–146.
[17] P. Spiesz, Q.L. Yu, H.J.H. Brouwers, Development of cement-based lightweight composites–Part 2: Durability-related properties, Cem. Concr. Compos. 44 (2013) 30–40.
[18] J. Lindgård, Ö. Andiç-Çakır, I. Fernandes, T.F. Rønning, M.D. Thomas, Alkali–silica reactions (ASR): literature review on parameters influencing laboratory performance testing, Cem. Concr. Res. 42 (2) (2012) 223–243.
[19] A. Mladenović, J.S. Šuput, V. Ducman, A.S. Škapin, Alkali-silica reactivity of some frequently used lightweight aggregates, Cem. Concr. Res 34 (2004) 1809–1816.
[20] Y. Matsuda, T. Tsuyoshi, T. Ishibashi, Investigation of real structures using lightweight concrete. In: Upgrade symposium on concrete repair and reinforcement, Kyoto, Japan, 2004, pp. 183–188.
[21] C. Shi, Z. Shi, X. Hu, R. Zhao, L. Chong, A review on alkali-aggregate reactions in alkali-activated mortars/concretes made with alkali-reactive aggregates, Mater. Struct. 48 (2015) 621–628.
[22] M.N.N. Khan, P.K. Sarker, Alkali silica reaction of waste glass aggregate in alkali activated Fly ash and GGBFS mortars, Mater. Struct. 52 (5) (2019) 93.
[23] A. Hajimohammadi, T. Ngo, A. Kashani, Glass waste versus sand as aggregates: the characteristics of the evolving geopolymer binders, J. Clean. Prod. 193 (2018) 593–603.
[24] P. Duxson, A. Fernández-Jiménez, J.L. Provis, G.C. Lukey, A. Palomo, J.S.J. Van Deventer, Geopolymer technology: the current state of the art, J. Mater. Sci. 42 (2007) 2917–2933, https://doi.org/10.1007/s10853-006-0637-z.
[25] J. Davidovits, Geopolymers: Ceramic-like inorganic polymers, J. Ceram. Sci. Technol. 8 (2017) 335–350, https://doi.org/10.4416/JCST2017-00038.
[26] N.B. Singh, B. Middendorf, Geopolymers as an alternative to portland cement: an overview, Constr. Build. Mat. 237 (2020) 117455, https://doi.org/10.1016/j.conbuildmat.2019.117455.
[27] P. Zhang, Y. Zheng, K. Wang, J. Zhang, A review on properties of fresh and hardened geopolymer mortar, Comp. Part B 152 (2018) 79–95, https://doi.org/10.1016/j.compositesb.2018.06.031.
[28] J.L. Provis, Alkali-activated materials, Cem. Con. Res. 114 (2018) 40–48, https://doi.org/10.1016/j.cemconres.2017.02.009.
[29] J.L. Provis, P. Duxson, J.S.J. van Deventer, The role of particle technology in developing sustainable construction materials, Adv. Powder Technol. 21 (2010) 2–7, https://doi.org/10.1016/j.apt.2009.10.006.
[30] ACI 211.2, Standard practice for selecting proportions for structural lightweight concrete, American Concrete Institute, 1998 (Reapproved 2004).
[31] ACI 213R, Guide for structural lightweight aggregate concrete, in: J.A. Bogas, A. Gomes (Eds.), A simple mix design method for structural lightweight aggregate concrete. Materials and Structures, 46, American Concrete Institute, Farmington Hills, 2003–2013, pp. 1919–1932.
[32] Maage M., Smeplass S., Thienel K. (2000) Structural LWAC specification and guideline for materials and production. In: Helland et al (eds.) Second international symposium on structural lightweight aggregate concrete, 18–22 June, Kristiansand, pp 802–810.
[33] D.M.A. Huiskes, A. Keulen, Q.L. Yu, H.J.H. Brouwers, Design and performance evaluation of ultra-lightweight geo-polymer concrete, Mat. Des. 89 (2016) 516–526, https://doi.org/10.1016/j.matdes.2015.09.167.
[34] R.H. Kupaei, U.J. Alengaram, M.Z.B. Jumaat, H. Nikraz, Mix design for Fly ash based oil palm shell geopolymer lightweight concrete, Constr. Build. Mat. 43 (2013) 490–496, https://doi.org/10.1016/j.conbuildmat.2013.02.071.
[35] E. Vasanelli, S. Calò, A. Cascardi, M.A. Aiello, The use of lightweight aggregates in geopolymeric mortars: the effect of liquid absorption on the Physical/Mechanical properties of the mortar, Materials 17 (8) (2024) 1798.
[36] F. Longo, P. Lassandro, A. Moshiri, T. Phatak, M.A. Aiello, K.J. Krakowiak, Lightweight geopolymer-based mortars for the structural and energy retrofit of buildings, En. Build. 225 (2020) 110352, https://doi.org/10.1016/j.enbuild.2020.110352.
[37] UNI EN 1015 – 3 2007, Methods of test for mortar for masonry – Part 3: Determination of consistence of fresh mortar (by flow table).
[38] Q.L. Yu, P. Spiesz, H.J.H. Brouwers, Ultra-lightweight concrete: conceptual design and performance evaluation, Cem. Concr. Compos. 61 (2015) 18–28.
[39] UNI EN 1015-10:2007 Methods of test for mortar for masonry - Part 10: Determination of dry bulk density of hardened mortar.
[40] CEN EN 12504-4:2021. Testing concrete in structures - Part 4: Determination of ultrasonic pulse velocity.
[41] ASTM D2845–08 Standard Test Method for Laboratory Determination of Pulse Velocities and Ultrasonic Elastic Constants of Rock
[42] UNI EN 1015-11:2019 Methods of test for mortar for masonry - Part 11: Determination of flexural and compressive strength of hardened mortar.
[43] ASTM C518–21 Standard Test Method for Steady-State Thermal Transmission Properties by Means of the Heat Flow Meter Apparatus.

[44] *ISO 8301:1991 Thermal insulation - Determination of steady-state thermal resistance and related properties - Heat flow meter apparatus*.
[45] J. Xie, O. Kayali, Effect of initial water content and curing moisture conditions on the development of Fly ash-based geopolymers in heat and ambient temperature, Constr. Build. Mater. 67 (2014) 20–28.
[46] Y. Wang, X. Liu, W. Zhang, Z. Li, Y. Zhang, Y. Li, Y. Ren, Effects of Si/Al ratio on the efflorescence and properties of Fly ash based geopolymer, J. Clean. Prod. 244 (2020) 118852.
[47] M. Sitarz, I. Hager, M. Choińska, Evolution of mechanical properties with time of Fly-Ash-Based geopolymer mortars under the effect of granulated ground blast furnace slag addition, Energies 13 (5) (2020) 1135, https://doi.org/10.3390/en13051135.
[48] R. Ghosh, S.P. Sagar, A. Kumar, S.K. Gupta, S. Kumar, Estimation of geopolymer concrete strength from ultrasonic pulse velocity (UPV) using high power pulser, J. Build. Eng. 16 (2018) 39–44, https://doi.org/10.1016/j.jobe.2017.12.009.
[49] M.N. Hadi, H. Zhang, S. Parkinson, Optimum mix design of geopolymer pastes and concretes cured in ambient condition based on compressive strength, setting time and workability, J. Build. Eng. 23 (2019) 301–313.
[50] R.M. Waqas, F. Butt, X. Zhu, T. Jiang, R.F. Tufail, A comprehensive study on the factors affecting the workability and mechanical properties of ambient cured Fly ash and slag based geopolymer concrete, Appl. Sci. 11 (18) (2021) 8722.
[51] J. Temuujin, A. Van Riessen, R. Williams, Influence of calcium compounds on the mechanical properties of Fly ash geopolymer pastes, J. Hazard. Mater. 167 (1-3) (2009) 82–88.
[52] Girts Bumanis, D. Bajare, A. Korjakins, Mechanical and thermal properties of lightweight concrete made from expanded glass, J. Sustain. Archit. Civ. Eng. 2 (2013) 26–32, https://doi.org/10.5755/j01.sace.2.3.2790.
[53] F.A. da Silva Fernandes, S. Arcaro, E.F. Tochtrop Junior, J.C. Vald´es Serra, C. P. Bergmann, Glass foams produced from soda-lime glass waste and rice husk ash applied as partial substitutes for concrete aggregates, Process Saf. Environ. Prot. 128 (2019) 77–84, https://doi.org/10.1016/j.psep.2019.05.044.
[54] J. Khatib, A. Jefimiuk, S. Khatib, Flexural behaviour of reinforced concrete beams containing expanded glass as lightweight aggregates, Slovak J. Civ. Eng. 23 (2015) 1–7, https://doi.org/10.1515/sjce-2015-0017.
[55] S.Y. Chung, M. Abd Elrahman, D. Stephan, Effect of different gradings of lightweight aggregates on the properties of concrete, Appl. Sci. 7 (6) (2017) 585.
[56] J.L. Provis, J.S.J. van Deventer, in: R.T. AAM (Ed.), Alkali-activated Materials: State-of-the-art Report, Springer/RILEM, Berlin, 2013.
[57] W. Lee, J. Van Deventer, The interface between natural siliceous aggregates and geopolymers, Cem. Concr. Res. 34 (2004), 195e206.
[58] A. Siddika, A. Hajimohammadi, M.A.A. Mamun, R. Alyousef, W. Ferdous, Waste glass in cement and geopolymer concretes: a review on durability and challenges, Polymers 13 (13) (2021) 2071.
[59] S.Y. Chung, M. Abd Elrahman, D. Stephan, Effect of different gradings of lightweight aggregates on the properties of concrete, Appl. Sci. 7 (6) (2017) 585.
[60] M. Morsy, S. Alsayed, Y. Al-Salloum, T. Almusallam, Effect of sodium silicate to sodium hydroxide ratios on strength and microstructure of Fly ash geopolymer binder, Arab. J. Sci. Eng. 39 (6) (2014) 4333–4339.
[61] A. Passuello, E.D. Rodríguez, E. Hirt, M. Longhi, S.A. Bernal, J.L. Provis, A. P. Kirchheim, Evaluation of the potential improvement in the environmental footprint of geopolymers using waste-derived activators, J. Clean. Prod. 166 (2017) 680–689, https://doi.org/10.1016/j.jclepro.2017.08.007.
[62] L. Imtiaz, S. Kashif-ur-Rehman, W.S. Alaloul, K. Nazir, M.F. Javed, F. Aslam, M. A. Musarat,). Life cycle impact assessment of recycled aggregate concrete, geopolymer concrete, and recycled aggregate-based geopolymer concrete, Sust 13 (24) (2021) 13515, https://doi.org/10.3390/su132413515.
[63] C. Ouellet-Plamondon, G. Habert, Life cycle analysis (LCA) of alkali-activated cements and concretes. Handbook of Alkali-Activated Cements, Mortars and Concretes, Woodhead Publishing-Elsevier, Cambridge, 2014, pp. 663–686.